RSC Advances

ROYAL SOCIETY OF CHEMISTRY

www.rsc.org/advances

RSC Advances RSCPublishing

ARTICLE

Morphology and Properties of Porous Polyimide Films Prepared Through Thermally Induced Phase Separation

Zhonglun Li, Huawei Zou and Pengbo Liu

State Key Laboratory of Polymer Materials Engineering, Polymer Research Institute of Sichuan University, Chengdu 610065, China

Porous polyimides (PI) synthesized from 4,4'-oxydiphthalic anhydride (ODPA) and 4,4′-diaminodiphenyl ether (ODA) monomers are materials promising ultralow-dielectric constant. We report here a strategy toward engineering PI films of various porous textures using a small molecular phase dispersion agent, dibutyl phthalate (DBP), as porogen. In the presence of DBP, the ODPA-ODA poly(amic acid) solution, the precursor to PI, undergoes phase separation as N,N-dimethylacetamide (DMAc) solvent is slowly evaporated, forming spherical domains of DBP phase uniformly dispersed in the polyamidic acid matrix. Upon thermal imidization, a polyimide film with high porosity is attained after acetone extraction of DBP. It is demonstrated in this study that the porous texture of PI films can be readily engineered by tailoring the initial DBP content. The average pore size increases with increasing concentration of DBP, but was no larger than 6 μm. The PI film achieves a dielectric constant of 1.7 at an optimal porosity of 72%, This study examined the pore formation mechanism, the imidization chemistry, the surface morphology, the density, the thermal stability and mechanical properties of the formed porous PI films. Thermo-gravimetric analysis indicated that porous films retain the inherent exceptional thermal stability of polyimides, with thermal decomposition onset above 500 ℃ in nitrogen atmosphere.

1. Introduction

Polyimides (PIs) are among the most promising candidates as next-generation interlayer dielectric materials. The performance and reliability of this class of materials originate from their unique combination of physicochemical and mechanical properties, including excellent thermal stability, low dielectric constant, and

good adhesion.[1] Unfortunately, the dielectric constant of pristine PI materials (κ ~ 3.4 in 1 kHz - 1 MHz frequency region)[2] is too high for the increasing transmission speed of mobile devices.[2, 3-6] Current studies on lowering dielectric constant of polymer materials focus on primarily two strategies.

1) to modify chemical structures of the PI backbone and/or side chains.[4] Due to the low dipole moment and low polarizability of C-F bonds,[4,7-8] fluorination reportedly decreases the κ value of polyimides to 2.7~3.0.[9]

2) engineering high volume of voids (κ ~ 1 for air pockets[10]) into PI matrices. Reprecipitation of PI nanoparticles is a convenient technique to fabricate porous film.[11-13] The dielectric constant achieved using this method is 1.9.[13] Another approach for forming pores involves physical foaming process, wherein CO_2 was dissolved and nucleated to form bubbles in PI matrix.[10, 14-15] The dielectric constant of this porous film decreased to 1.77.[10] Nonsolvent and vapour-induced phase separation have been used to fabricate open-pore film.[16-19] Embedding hollow filler represents another approach in which inorganic porogens such as hollow silica particles and mesoporous silica added to the matrix to reduce the dielectric constant.[20] Etching of silica nanoparticles in a PI matrix by hydrofluoric acid could prepare film with dielectric constant of 1.84.[21-23] The sacrificial template method utilizes phase separation in a PI matrix. Subsequent thermolysis or extraction of labile block copolymer or blends creates pores in the film.[24-26] Many polymers, such as poly(methyl methacrylate) (PMMA),[26,27] polystyrene (PS),[28] poly(ethylene oxide) (PEO),[29-30] and poly(vinylpyrrolidone) (PVP),[31] could be used as porogen. Firstly these polymers are blended with poly(amic acid) (PAA, PI precursor) through solution blending. After imidization, these components are selectively degraded thermally or removed by extractants so as to form pores in the PI matrix. However, it is generally believed that the complete removal of porogen is challenging, if not entirely impossible.

Herein, we proposed a simple approach to prepare porous PI(Figure 1-a) film with low k values, by using a small molecule such as dibutyl phthalate (DBP，Figure 1-b), as porogen. DBP can be easily removed by common extractants. Firstly, a N,N-dimethyl acetamide (DMAc) solution of poly(amic acid) and DBP was casted on a glass substrate. A phase separation of DBP and poly(amic acid) occurs as solvent evaporates. After imidization, DBP was removed with acetone, resulting in a highly porous PI structure. By varying the porogen concentration in poly(amic acid) solution, PI films with various porous textures were obtained. The effects of porogen concentration on the morphology of the porous PI films were studied. The correlation of the pore structure and porosity to the performance of the films were also examined.

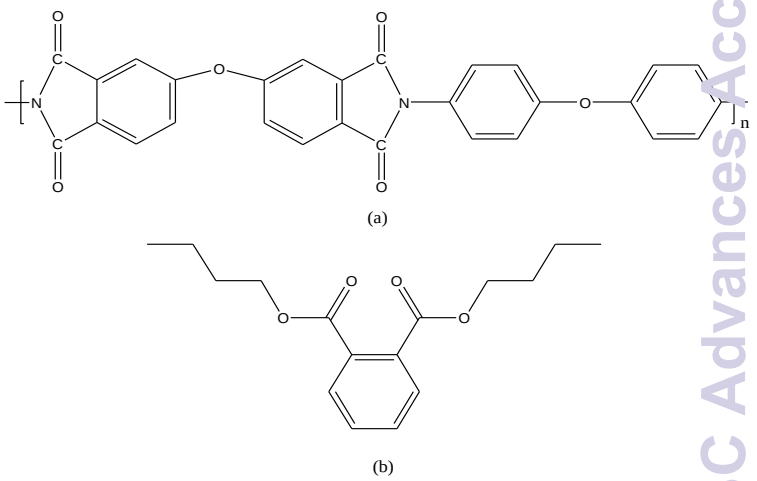

Figure 1 Chemical structure of (a) polyimide and (b) DBP.

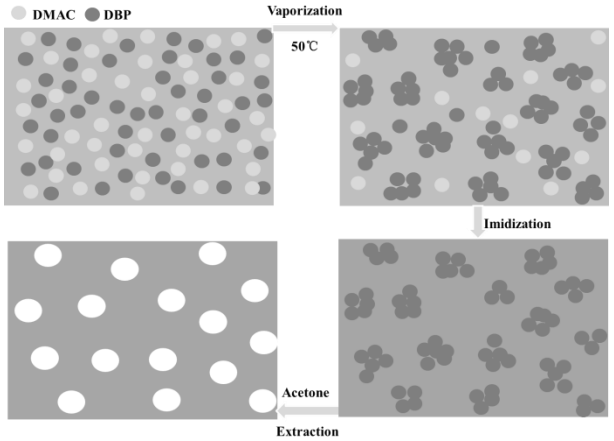

Figure 2 Schematic diagram of porous PI films formation from a solution of PAA and DBP.

2. Results and discussion

Preparation of porous PI films

Choice of porogen is essential to the final porous texture of PI films and the achievable κ values. DBP is a fairly nonpolar, low-κ organic compound. At the molecular level, DBP is not miscible with poly(amic acid) in a broad temperature range. Its low vapour pressure and good thermal stability in the imidization temperature regime renders an effective means to stabilize the DBP domains from which the final porous texture is derived.

PAA and DBP were co-dissolved in DMAc to form a homogeneous solution. The precursor film was prepared by casting the aforementioned solution onto a glass plate. As DMAc solvent slowly evaporates, DBP and PAA undergo a phase separation, evidenced by transformation of the initially transparent film into a turbid film. Figure 2 reveal formation of micron-size spherical DBP domains uniformly dispersed in PAA matrix. When heated to 50 ℃, spherical domains aggregate into large dispersed clusters. Following the thermal imidization, a porous structure was formed after the disperse phase was extracted out with acetone. The pore formation process was schematicly illustrated in Figure 2.

To assess imidization degree, films were analyzed by ATR FT-IR technique. Figure 3 compares the spectra of samples before and after thermal imidization. The characteristic absorption of amide groups (ν_s ~ 1656 cm^{-1}) and carboxylic groups (ν_s ~ 1711 cm^{-1}) in PAA, completely disappears after thermal imidization (Figure 3-a), while absorption bands corresponding to imide ring structures appears, including the asymmetric stretching (ν_{as} ~ 1777 cm^{-1}) and the symmetric stretching (ν_s ~ 1719 cm^{-1}) of the carbonyl group, and the stretching vibration of C-N in the imide ring (ν_s ~ 1375 cm^{-1}) and the weak absorption peak (δ ~ 744 cm^{-1}) from the imide ring deformation (Figure 3-b).[13] These results confirm that PAA has been successfully converted to polyimide by the thermal imidization process.

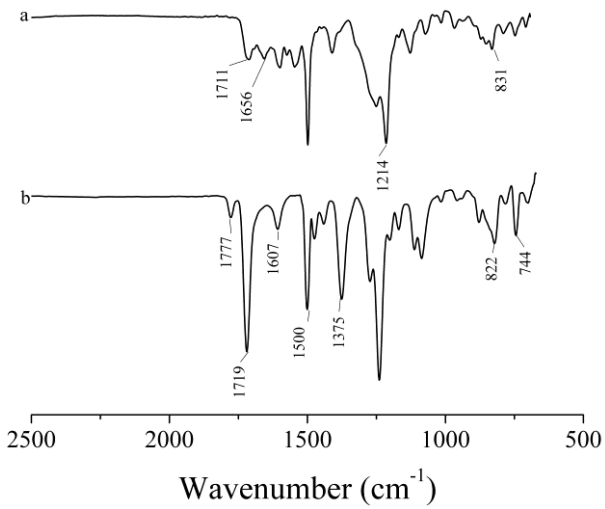

Figure 3 ATR-FTIR spectra of the cast PAA films before (a) and after (b) thermal imidization.

Effect of DBP concentration on pore structure evolution

Figure 4 shows the cross section SEM images of porous PI films prepared using 5 - 20 wt% DBP as phase dispersion agent. These

films are characterized with uniform distribution of closed pores. Most pores adopt a spherical or oval shape, geometries minimizing surface tension. Also, few cracked walls or fused pores are present. These findings indicate that at up to 20 wt% of DBP, the DBP/PAA system still favors forming discrete spherical domains of DBP embedded in the continuous PAA phase. The results also suggest that during solvent extraction of DBP, the PI skeleton is sufficiently robust to endure the surface tension change without collapsing pore walls.

The porous texture of PI films can be readily tailored by adjusting the porogen content. Figure 4 shows that at the increasing DBP content, individual pore size enlarges, accompanied by slight pore wall thinning, Figure 5 illustrates the correlation of average pore size and porosity of porous PI films with DBP content. High DBP concentration leads to pore enlargement as well as an increase in porosity. As the concentration of DBP in PAA solution increases from 5 wt% to 20 wt%, the average pore size expands from 3 μm to 6 μm, while the porosity increases from 12% to 70%. The thickness of the porous PI films also increases with DBP concentration because of more pores formed in each film of the same quality. As the concentration of DBP in PAA solution increases from 5 wt% to 10 wt%，the obvious jump in obtained porosity might be caused by more easier phase separation of DBP. This phenomenon suggests the efficiency of forming additional DBP domains decreases as DBP concentration increases.

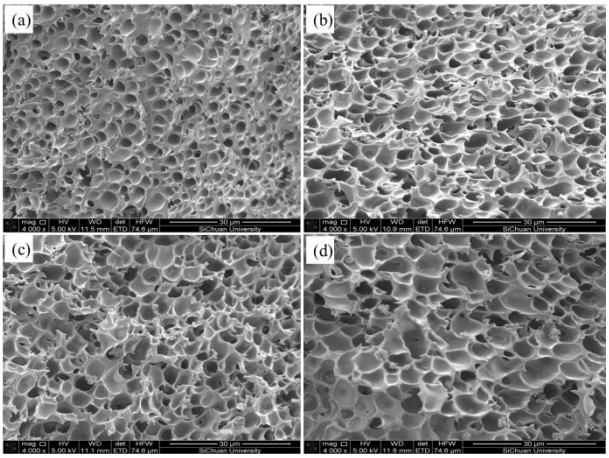

Figure 4 SEM images of cross-section of porous PI films prepared at: (a) 5 wt% DBP, (b) 10 wt% DBP, (c) 15 wt% DBP and (d) 20 wt% DBP.

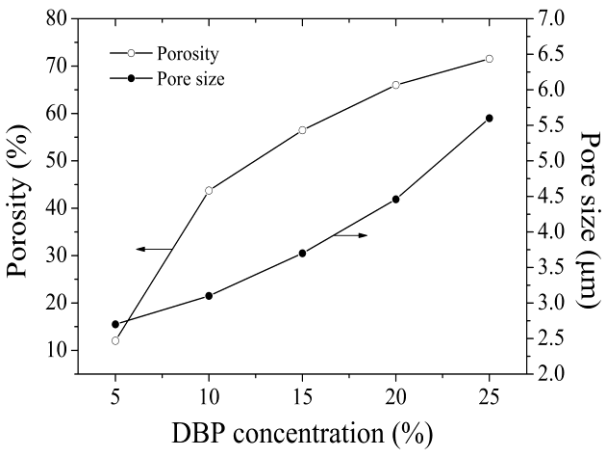

Figure 5 Effect of DBP concentration on the porosity and average cell size of porous PI films.

Properties of porous PI films

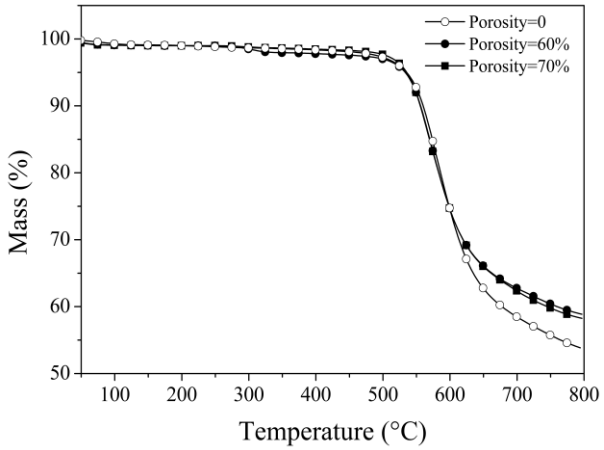

Figure 6 TGA curves of porous PI films.

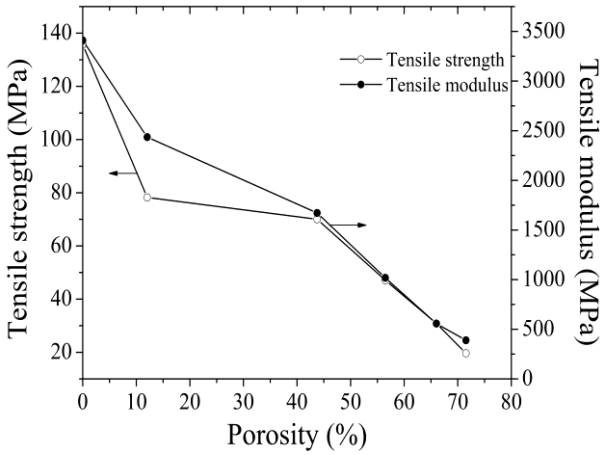

Figure 7 Influence of porosity on the tensile strength and tensile modulus of porous PI film.

Table 1 TGA data of porous PI films

Porosity (vol%)	0	55	70
$T_{5\%}$ (℃)	538	535	536
$T_{10\%}$ (℃)	557	557	557

$T_{5\%}$: Temperature at 5 wt% weight loss; $T_{10\%}$: Temperature at 10 wt% weight loss.

The residual DBP content and thermal stability of the porous PI films were evaluated with TGA technique. Figure 6 shows the TGA curves of dense and porous PI films. The dense PI film was fabricated following the same procedure, without addition of DBP as dispersion agent. The porous films exhibit similar thermal stability to the dense PI film, with major thermal decomposition occurring at 530 °C – 600 °C in the inert atmosphere. Porous films do not show obvious weight loss nearby 340 °C (boiling point of DBP). These observations indicate that the current pore-formation mechanism enables effective removal residual porogen molecules_from the PI matrix. The decomposition temperatures of the samples are listed in Tale 1. $T_{5\%}$ (temperature at 5 wt% weight loss) and $T_{10\%}$ (temperature at 10 wt% weight loss) of the nonporous PI film and porous PI films are almost same, further confirming that the porous PI films retain the excellent thermal stability of polyimide.

The mechanical properties of porous PI films were evaluated by tensile test. Figure 7 shows the influence of porosity on the tensile strength and tensile modulus of the porous PI films. Tensile strength and tensile modulus of the dense PI film are 135 MPa and 3400 MPa, respectively. Porous films exhibit reduced tensile strength and tensile modulus as the porosity increases following a nearly linear trend. At 70% porosity, the tensile strength and tensile modulus of the porous film dropped to 23 MPa and 500 MPa, respectively. Stress concentration in the vicinity of pores, and the reduced section area are believed to be largely responsible for the decreased tensile strength and modulus of porous films.[13]

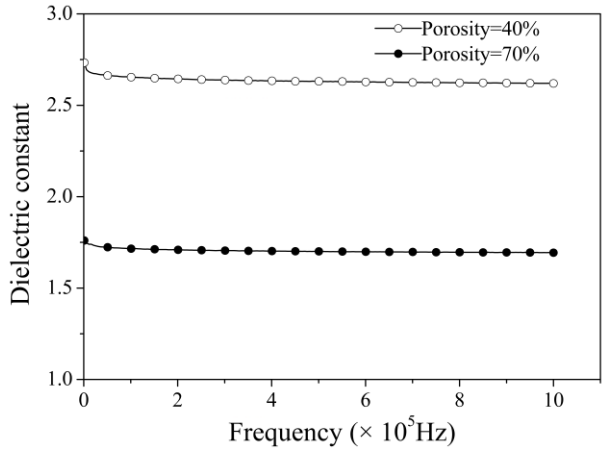

Figure 8 Frequency dependence of the dielectric constant of porous PI films.

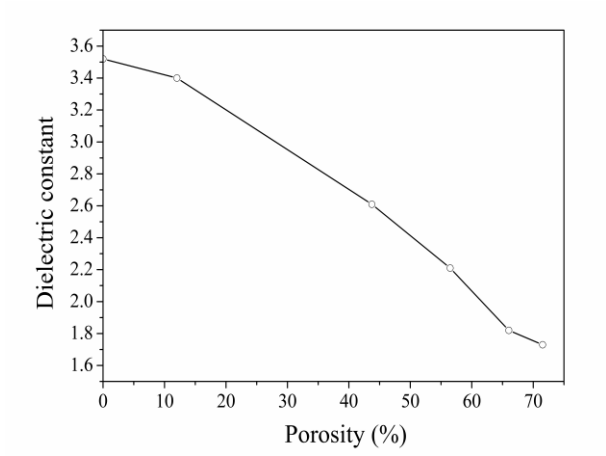

Figure 9 Influence of porosity on the dielectric constant of the porous PI film.

The influence of frequency on the dielectric constant of the porous PI films was investigated using an impedance analyzer in the frequency range of 1 kHz to 1 MHz (Figure 8). The dielectric constant of the porous films exhbits a slight decrease in the low frequency range, but remains unchanged in the frequency range of 1 kHz to 1 MHz.

Figure 9 shows the influence of the porosity on the dielectric constant at 1 MHz. The dielectric constant of the dense PI film was 3.52. In comparison, porous PI films exhibit considerably lower dielectric constants. It is also observed that the dielectric constant of the porous PI films decreases almost proportionally as the porosity increases. At the porosity of 70%, the dielectric constant of the porous film reaches $\kappa \sim 1.7$. These observations are in line with the fact that incorporation of air voids ($\kappa \sim 1$) into the PI matrix can effectively reduce the dielectric constant of materials.[10]

Experimental

Materials

Poly(amic acid) solution (SK-0910) is a DMAc solution containing 20% solid content. This PI precursor solution was purchased from Changzhou Sunchem High Performance Polymer Co. Ltd. (Changzhou, China). The PI was synthesized from 4,4'-oxydiphthalic anhydride (ODPA) and 4,4′-diaminodiphenyl ether (ODA). The chemical structure of PI [p(ODPA-ODA)] after imidization is depicted in Figure 1-a. Dibutyl phthalate (DBP), supplied by Chengdu KeLong Chemical Co. Ltd. (Chengdu, China), was used as porogen and its chemical scheme is also shown in Figure 1-b. DMAc and acetone, supplied by Chengdu KeLong Chemical Co. Ltd., were used as solvent and extractant, respectively. All agents were used as received without further purification.

Preparation of porous PI films

In a 150 mL three-necked round-bottomed flask fitted with a mechanical stirrer, 3.5 g poly(amic acid) solution was added, certain amount of DBP and DMAc was also added in order to prepare mixture with different DBP concentration of 5, 10, 15, 20 and 25 wt%, respectively. For every sample, poly(amic acid) concentration is always 14 wt%. The mixture was stirred for 1 h at room

temperature in nitrogen atmosphere to form a homogeneous solution. Approximately 200 μm thick thin films were solution casted on a glass plate using a drawknife. The casted films were allowed to dry in nitrogen atmosphere at 50 ℃ for 2 h to evaporate DMAc solvent and induce phase separation. Subsequently, the composite film was consecutively heated at 100 ℃ for 1 h, 150 ℃ for 1 h, 200 ℃ for 1 h and 250 ℃ for 1 h in order to convert the poly(amic acid) to polyimide. After imidization, DBP porogen in the films were extracted with 100 ml acetone three times at room temperature. After extraction, the film was further dried in a vacuum oven at 80 ℃. The film thickness was measured with a digital caliper.

Measurements and characterization

Attenuated total reflection Fourier transform infrared (ATR-FTIR) spectra of the samples were recorded on a Nicolet-560 FTIR spectrometer (Nicolet Corp., U.S.A) in the wavenumber range of 2500~500 cm^{-1}.

Density of the film samples was assessed by a GH-128E electronic solid density instrument (Xi Men Qunlong Instruments, China), which is based on Archimedes' principle. Porosity of the samples was calculated from the relative density (obtained as the ratio between the density of the porous (ρ_f) and the solid (ρ_s) material) using following equation.[32]

$$\text{Porosity} = 1 - \frac{\rho_f}{\rho_s} \qquad (1)$$

Morphology of the samples was evaluated with a scanning electron microscope (Quanta250，FEI instrument, USA). Samples were frozen in liquid nitrogen and fractured. The cross sections of fractured samples were sputter-coated using gold in argon with sputtering current of 18 mA for 90 seconds by a sputter coater (SC7620, Quorum) and eventually thickness of the sputtering layer was 275 Å The micrographs obtained were used to analyse pore size and its distribution.[33]

Thermo-gravimetric analysis (TGA) was conducted on a Q600 TGA analyzer (TA Instruments, U.S.A) at a heating rate of 10 K/min, and nitrogen flow rate 50 mL/min.

Tensile strength and tensile modulus were measured using an INSTRON 5567 universal testing machine (Instron Corp., U.S.A) at a crosshead speed of 3 mm/min according to the Chinese National Standard GB/T13022-91. For each data of mechanical properties, five specimens were measured.

The dielectric properties were measured using an Agilent 4294A precision impedance analyzer (Agilent Technologies, U.S.A). The 1×1 cm^2 specimens were cut from the PI films. Au was sputtered on the both sides of the specimens, which acted as electrode. The probes were connected with Au electrodes, then the capacitance (C_p) of the specimens were measured at 500 mV under ambient condition, in the frequency from 100 Hz to 1 MHz. The dielectric constant was calculated using the following equation.

$$\kappa = \frac{C_p d}{\kappa_0 S} \qquad (2)$$

Where κ is the dielectric constant, κ_0 is the permittivity of the free space (8.85×10^{-12}MKS unit), d is the thickness of the sample, and S is the area of the sample.

3. Conclusion

An effective and simple process is demonstrated for fabricating porous PI films achieving extreme low dielectric constant. DBP is chosen as the porogen based on the following consideration: 1) low polarity hence immiscible with the PI precursor solution PAA,

which is favourable for forming stable μm-size spherical domains uniformly dispersed throughout the PAA matrix; 2) high boiling point, low vapour pressure and good thermal stability at the imidization temperature, which enables direct control of porous textures similar to polymer-based porogen; and 3) easily extracted by common solvent leaving practically no residual porogen in the formed porous film. The as prepared porous PI films achieve dielectric constant of 1.7, and exhibits excellent thermal stability. At a porosity of 70%, the porous PI film achieves dielectric constant of 1.7 across the frequency range of 1 kHz to 1 MHz, which renders these materials a potential candidate for ultralow dielectric constant applications.

References

1 G. Zhao, I. Takayuki, K. Hitoshi, O. Hidetoshi, N. Hachiro, *Chem. Mater.*, 2007, **19**, 1901.

2 J. O. Simpson, A. K. Clair St, *Thin Solid Films* 1997, **308**, 480.

3 M. H. Weng, H. W. Wu, Y. K. Su, R. Y. Yang, C. Y. Hung, *Microw. Opt. Techn. Let.*, 2006, **48**, 1675.

4 H. W. Wu, Y. K. Su, R. Y. Yang, M. H. Weng, Y. D. Lin, *Microelectr. J.*, 2007, **38**, 304.

5 Y. Ren, D. C. C. Lam, *J. Electron. Mater.*, 2008, **37**, 955.

6 X. Y. Zhao, H. J. Liu, *Polym. Int.*, 2010, **59**, 597.

7 W. Volksen, R. D. Miller, G. Dubois. *Chem. Rev*. 2010, **110**, 56.

8 M. M.Unterlass, D. Kopetzki, M. Antonietti, J. Weber. *Polym. Chem.*, 2011, **2**, 1744.

9 K. Taki, K. Hosokawa, S. Takagi, H. Mabuchi, M. Ohshima, *Macromolecules*, 2013, **46**, 2275.

10 B. Krause, G. H. Koops, N.F. van der Vegt, M. Wessling, M. Wubbenhorst, J. van Turnhout, *Adv. Mater.*, 2002, **14**, 1041.

11 G. Zhao, T. Ishizaka, H. Kasai, H. Oikawa, H. Nakanishi, *Mol. Cryst. Liq. Cryst.* 2007,**464**,613.

12 G. Zhao, T. Ishizaka, H. Kasai, M. Hasegawa, H. Nakanishi, H. Oikawa, *Polym. Adv.Technol.*, 2009, **20**, 43.

13 G. Zhao, T. Ishizaka, H. Kasai, M. Hasegawa, T. Furukawa, H. Nakanishi, H. Oikawa, *Chem. Mater.*, 2009, **21**, 419.

14 M. Hasegawa, K. Horie, *Prog. Polym. Sci.*, 2001, **26**, 259.

15 B. Krause, K. Diekmann, N. F. A. van der Vegt, M. Wessling, Macromolecules 2002, 35, 1738 −1745.

16 L. Y. Pan, M. S. Zhan, K. Wang, *Polym. Eng.Sci.*, 2010, **50**,1261.

17 H. Wang, T. Wang, S. Yang, L. Fan *Polymer*. 2013, **54**, 6339.

18 S. Kim, K. S. Jang, H. D. Choi, S. H. Choi, S. J. Kwon, I. D. Kim, J. M. Hong, *In. J. Mol. Sci.*, 2013, **14**, 8698.

19 L. Wang, Y. Tian, H. Ding, B. Liu, *Eur. Polym. J.*, 2007, **43**, 862.

20 A. E. Eichstadt, T. C. Ward, M. D. Bagwell, I. V. Farr, D. L. Dunson, J. E. McGrath, *Macromolecules*, 2002, **35**, 7561.

21 L. Z. Jiang, J. G. Liu, D. Z. Wu, H. G. Li, R. G. Jin, *Thin Solid Films*, 2006, **510**, 240.

22 P. Musto, G. Ragosta, G. Scarinzi, L. Mascia, *Polymer* 2004, **45**, 1697.

23 C. J. Cornelius, E. Marand, *Polymer* 2002, **43**, 2385.

24 F. Z. Lv, L. P. Liu, Y. H. Zhang, P. G. Li, *J. Appl. Polym. Sci.*, 2015, **132**, 41480.

25 K. R. Carter, R. A. DiPietro, M. I. Sanchez, T. P. Russell, *Chem.Mater*.,1997, **9**,105.

26 H. Z. Zhou, M. S. Zhan, K. Wang, X. Y. Liu, *High. Perform. Polym*., 2012, **25**,33.

27 G. D.Fu, B. Y. Zong, E. T. Kang, *Ind. Eng. Chem. Res*.,2004, **43**, 6723.

28 T. M. Wang, Q. H. Wang, *Express. Polym. Lett.*, 2013, **7**, 667.

29 Y. J. Lee, J. M. Huang, S. W. Kuo, F. C. Chang, *Polymer*, 2005, **46**, 10056.

30 Y. H. Zhang, L. Yu, L. H. Zhao, W. S. Tong, H. T. Huang, S.M. Ke, *J. Electron. Mater*., 2012, **41**,2281.

31 (a) C. P. Yang, Y. Y. Su, H. C. Chiang, *React. Funct. Polym.*, 2006, **66**, 689; (b)J. C. Huang, C. B. He, Y. Xiao, K. Y. Mya, J. Dai, Y. P. Siow, *Polymer*, 2003, **44**, 4491.

32 J. Kwon, J. Kim, D. Park, *Polymer*, 2015, **56**, 68.

33 M. D. Abramoff, P. J. Magelhaes, S. J. Ram, *J. Biophotonics. Int.*, 2004, **11**, 36.